

FIELD AND NUMERICAL STUDIES ON THE WIND-INDUCED INTERNAL OSCILLATION IN A RESERVOIR

By

Morimasa Ohtani, Keiji Okamura

and

Isao Yakuwa

Department of Engineering Science, Hokkaido University
North 13, West 8, Sapporo 060, Japan.

SYNOPSIS

Behavior of the internal oscillation due to the wind force is studied in this paper on the basis of the observed results of the water temperature at Kanayama Reservoir. Moreover, numerical analysis using a two-layer model is applied to this problem.

From the water temperature changes, it is found that the internal oscillations at the upstream and downstream station have slightly different amplitude and period. At the station near the dam where the water depth is about 35m, the depth of the thermocline changes between 3m and 5m with the period of 23hr 13min. On the other hand, at the station near the end of the reservoir where the water depth is shallower (about 12m), the depth changes from 5m to the whole depth of water with the period of 21hr 15min. At this station, the water temperature of the upper and lower layer becomes nearly equal when the strong wind flows in upstream direction.

These periods of the internal oscillation are both longer compared with the calculated natural periods (17hr 03min at Sta. 1 and 18hr 57min at Sta. 3) of the internal seiche, and nearly equal to the periods of the wind speed observed at respective stations; 23hr 16min and 21hr 20min.

Accordingly, it seems that the internal oscillation is mainly caused by the set-up induced by the wind force.

INTRODUCTION

It is well known that a thermocline in the lake or the reservoir is formed by mainly solar radiation. Wind action upon the thermal stratification causes surface seiche, internal seiche and circulation flow. Such phenomena have been studied experimentally and theoretically by many researchers. For instance, Mortimer(6) discussed the depth of the thermocline influenced by the flow due to the wind force and Heaps and Ramsbottom(3) studied the wind induced internal seiche using a response function of a long wave. Kanari(5) showed the existence of a rotational Kelvin wave and an internal Poincaré wave in the lake. Furthermore, Fukushima and Muraoka(1) observed and studied numerically the seiche in the shallow lake and Furumoto et al.(2) introduced formula to express a development of the internal seiche induced by the wind stress. Recently, Muraoka and Hirata(7) used the Holmboe's model to account for the period of the internal seiche and Imberger(4) discussed the vertical distribution of the water temperature in the upper layer of the lake which was influenced by the wind force. However, only a few reports on field observations of the phenomena have been presented.

In order to study a relation between the internal oscillation and the wind in the reservoir, the authors measured water temperature, wind speed and wind direction at three stations of Kanayama Reservoir during a period from August 8 to August 19, 1985. We show the data sets obtained in this observation and discuss about the origin of the internal oscillation using the calculated results based on the two-layer model.

The Kanayama Reservoir, located in the central part of the Hokkaido, was formed by damming up the Sorachi River which is the tributary river of the Ishikari River and has a length of about

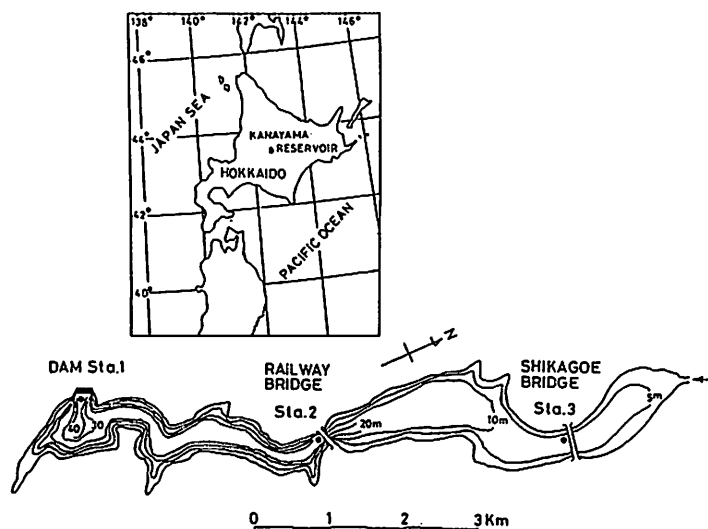


Fig.1 Location and topography of Kanayama Reservoir.

Table1 Morphological data of Kanayama Reservoir.

Surface area	9.2km ²
Effective capacity	150.45 × 10 ⁶ m ³
Height of dam	57.3m
Length of crest	288.5m
High water level	EL 345.0m
Low water level	EL 320.0m

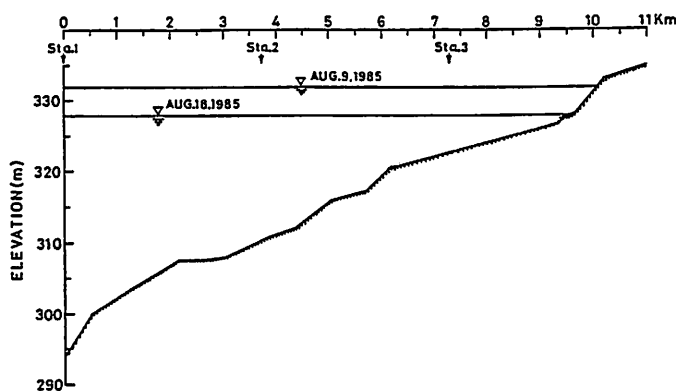


Fig.2 Longitudinal profile of the bottom and water level on 9 and 18 August, 1985.

195km. The reservoir has a total storage capacity of $150 \times 10^6 \text{ m}^3$ and it is used for flood control, irrigation and water-power generation. Figure1 shows location map and topography of Kanayama Reservoir and Table1 indicates its morphological data. The longitudinal profile of the bottom of this reservoir is shown in Fig.2 with the water levels on 9 and 18 August.

FIELD OBSERVATION

Two thermocouple type thermometer chains were settled about 30m off the dam (Sta.1) and at Shikagoe Bridge, 7.2km upstream from the dam (Sta.3). The chain was set vertically on the bottom by an anchor and a buoy so that the depth of each sensor from the water surface was constant. The water temperature was measured at intervals of 0.5m from the surface to 10m in depth, at 1.0m

intervals from 10 to 15m and at 2m intervals from 15 to 20m respectively. At a middle point, 3.7km upstream from the dam and 20m off the right bank (Sta.2), the water temperature was observed by thermistor thermometer at the surface and four points 1m, 3m, 5m and 7m in depth. At each station, the water temperature was recorded by digital recorder at intervals of 30 min. Wind speed and wind direction were measured by propeller-type anemometer at Sta.1 and Sta.3, and recorded there.

Figure 3 indicates the yearly change of the water level and isotherms in 1985. From this figure, a level change of about 13.0m can be seen through the year and a drop of the level reaches about 30cm/day in the middle of August. The reservoir is strongly stratified in the summer season and the most stable stratification is observed at a period from the late of July to the late of August. A shaded part shows the period when the observation was carried out.

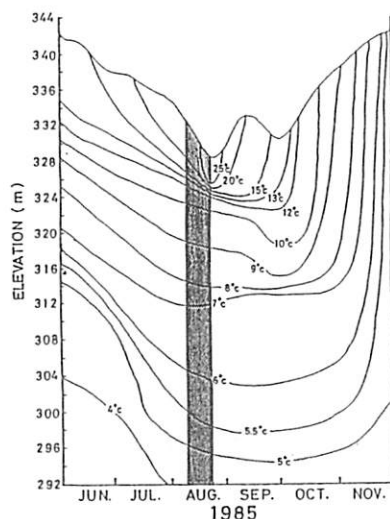


Fig. 3 Seasonal changes of surface level and isothermal lines.

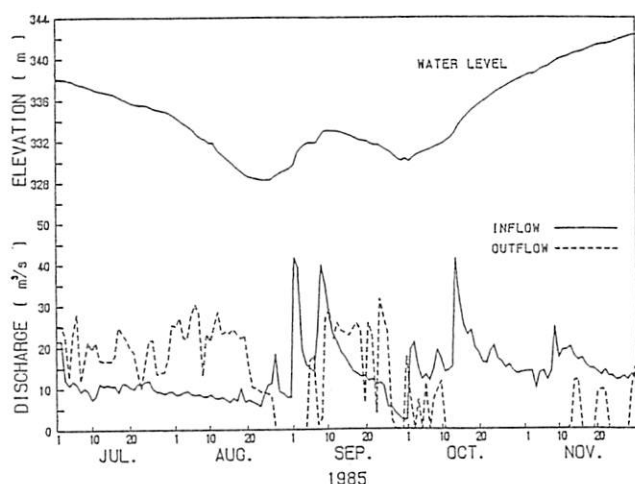


Fig. 4 Hydrological records from July to November, 1985.

The changes of the water level, inflow and outflow discharge from July to November are shown in Fig. 4. The river water flows into the reservoir at its end and the outlet near the dam is controlled to let the water of the surface layer out. In order to examine the influence of the inflow and outflow on the flow in the reservoir, we tried to measure the flow velocity by the electromagnetic current meter of sensitivity 1cm/s at Stations 1, 2 and 3 but the flow could not be detected by the current meter at every station. Therefore, the influence is treated as negligibly small in the following study.

Figure 5 shows the water temperature change in the layer from the surface to the 10m depth at Sta. 1 and Sta. 3 during the observational period. Although the change at the surface layer is induced by the meteorological conditions, its amplitude is smaller compared with the inner part of the stratified layer. At Sta. 1, the amplitude of the water temperature fluctuation reaches more than 10°C near the thermocline whose depth is about 4m. At Sta. 3, the depth of the thermocline is deeper and the maximum amplitude of the temperature fluctuation is larger as compared to Sta. 1. These water temperature fluctuations are presumably due to the internal oscillation, because its amplitude is maximum near the interface and becomes smaller with increase of the depth. The temperature fluctuation at Sta. 2 was observed in phase to Sta. 1, but out of phase to Sta. 3.

Figure 6 shows the typical daily changes of the vertical distribution of the water temperature at Sta. 1 and Sta. 3 from 11 to 14 August in the observational period. At Sta. 1 where the water depth is about 35m, the depth of the thermocline changes between 3m to 5m and the water temperature of the upper and lower layer does not change. On the other hand, at Sta. 3 where the depth is about 12m, the depth of the thermocline changes from 5m to the whole depth of water. On August 12 when the strong wind of maximum speed 13m/s blew from the dam in upstream direction, the water temperature of the lower layer became nearly equal to the upper layer from 6:00 to 12:00.

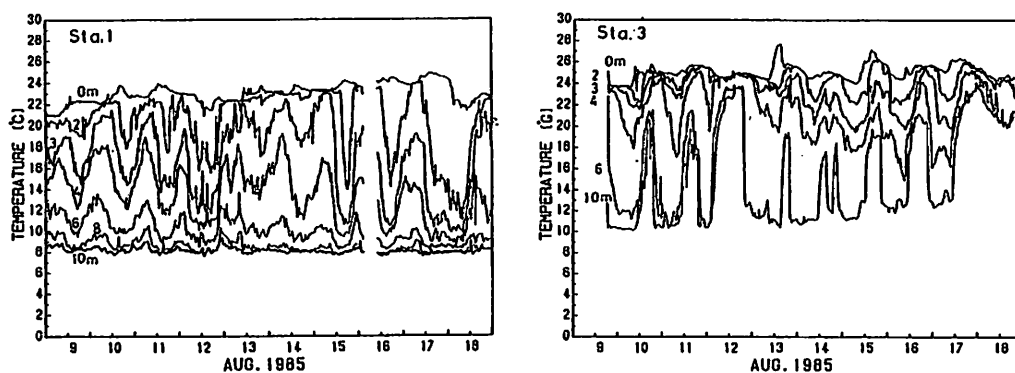


Fig. 5 Changes of water temperature at Sta. 1 and Sta. 3, from 9 to 18 August, 1985.

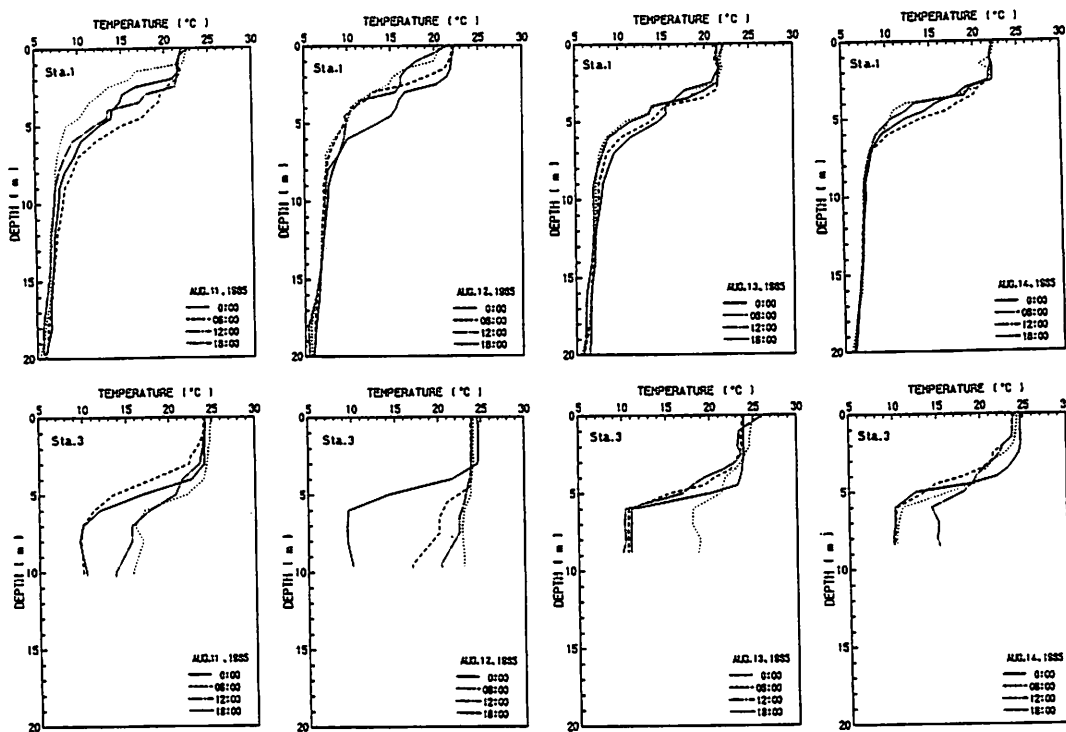


Fig. 6 Vertical distributions of water temperature at Sta. 1 and Sta. 3, from 11 to 14 August, 1985.

Figures 7 and 8 show the changes of the wind speed and the isothermal lines at Sta. 1 and Sta. 3. The wind direction is taken as SW when the wind blows from the dam in upstream direction and the opposite direction as NE. In the periods from 9 to 12 and from 16 to 17, the strong SW wind and NE wind blew periodically with a period of about 20 hours. The mean values of the wind speed were observed as 4.0m/s(SW) and 0.2m/s(NE) at Sta. 1, 4.7m/s(SW) and 0.2m/s(NE) at Sta. 3 respectively in the former period, 4.2m/s(SW) and 0.5m/s(NE) at Sta. 1, 5.1m/s(SE) and 0.4m/s(NE) at Sta. 3 in the latter period. The maximum speed of SW wind was observed on

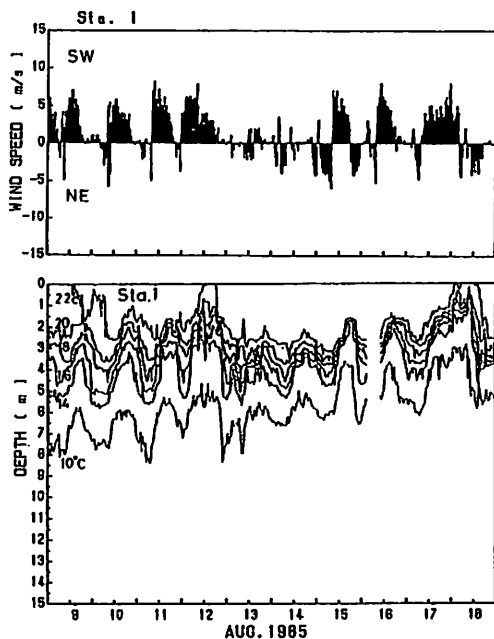


Fig. 7 Changes of wind speed and water temperature at Sta. 1 .

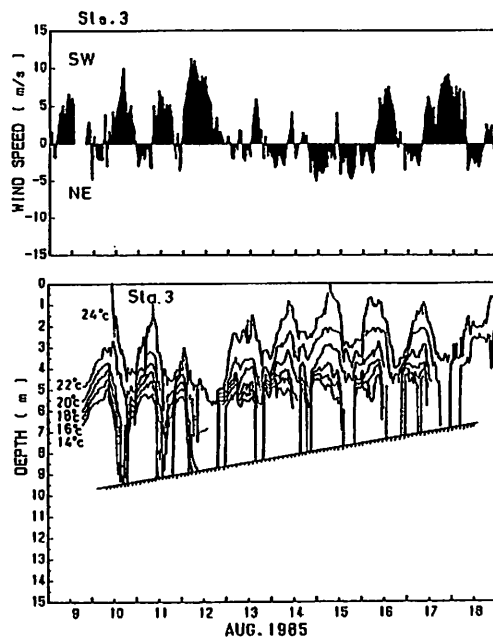


Fig. 8 Changes of wind speed and water temperature at Sta. 3 .

12 August as 10.0m/s at Sta. 1 and 12.7m/s at Sta. 3 . Isothermal lines in these figures were obtained by the linear interpolation from the records shown in Fig. 5 . It is found that the isothermal lines fluctuate periodically corresponding to the change of the wind speed.

Figures 9 and 10 are the results of spectral analysis of the water temperature and wind speed. Data of the temperature and wind speed recorded at Sta. 1 and Sta. 3 were analyzed by the FFT method, where the data at 512 points with interval of 30min were used. In the spectral analysis, the SW and NE wind was taken as + and - respectively and the low-cycle component in the isothermal line was eliminated by linear approximation. The periods of water temperature variation; 23hr 13min (Sta. 1) and 21hr 15min (Sta. 3) are nearly equal to the wind periods; 23hr 16min (Sta. 1) and 21hr 20min (Sta. 3) respectively. These results show that the change of the water temperature is largely influenced by the wind.

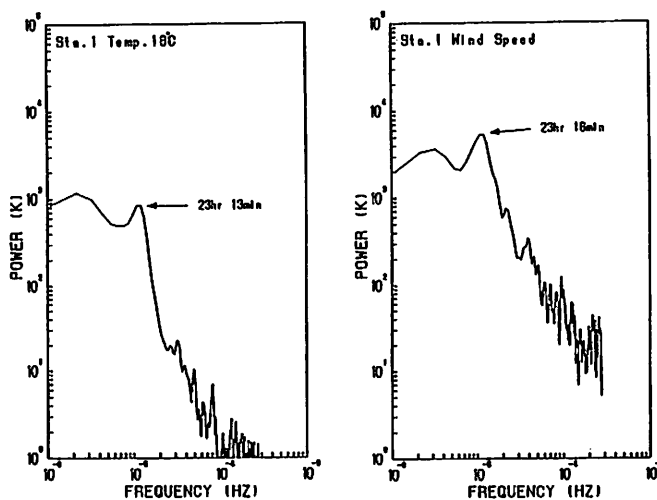


Fig. 9 Spectra of isothermal line of water temperature 18°C and wind speed at Sta. 1 .

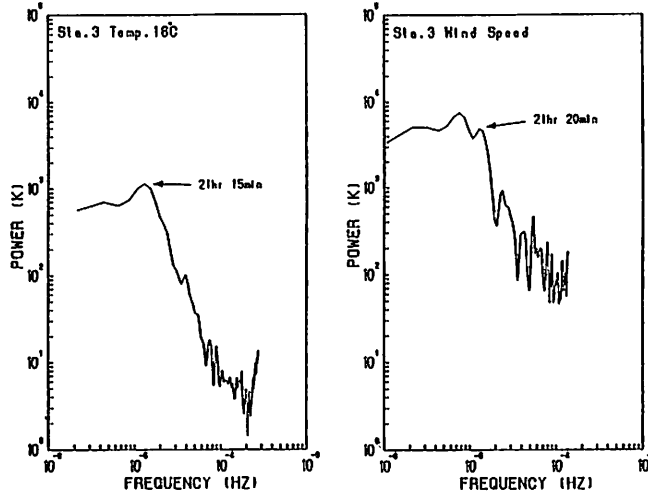


Fig. 10 Spectra of isothermal line of water temperature 18°C and wind speed at Sta. 3 .

NUMERICAL CALCULATION BY TWO-LAYER MODEL

(1) Comparison with observed results

A numerical calculation was carried out in order to make clear the influence of the water depth, the reservoir shape and the wind action on the internal oscillation. A two-layer model suggested by Kanari(5) was used in this study.

Let the density of water in the upper and lower layer ρ_1 and ρ_2 respectively. The x and y coordinates are taken horizontally on the surface and z coordinate vertically upwards to x - y plane. When the vertical pressure is assumed to be hydrostatic, the following linearized equations of motion can be obtained after integrating over the upper and lower layer ;

$$\left. \begin{aligned} \frac{\partial \bar{u}_1}{\partial t} &= -gh_1 \frac{\partial \eta_s}{\partial x} + \frac{1}{\rho_1} (\tau_s)_x \\ \frac{\partial \bar{v}_1}{\partial t} &= -gh_1 \frac{\partial \eta_s}{\partial y} + \frac{1}{\rho_1} (\tau_s)_y \\ \frac{\partial \bar{u}_2}{\partial t} &= -(1-\epsilon)g(H-h_1) \left[\frac{\partial \eta_s}{\partial x} + \epsilon \frac{\partial \eta_i}{\partial x} \right] - \frac{1}{\rho_2} (\tau_b)_x \\ \frac{\partial \bar{v}_2}{\partial t} &= -(1-\epsilon)g(H-h_1) \left[\frac{\partial \eta_s}{\partial y} + \epsilon \frac{\partial \eta_i}{\partial y} \right] - \frac{1}{\rho_2} (\tau_b)_y \end{aligned} \right\} \quad (1)$$

in which H is the water depth, h_1 the mean depth of the upper layer, η_s and η_i are the level of surface and interface, ϵ means $\epsilon = (\rho_2 - \rho_1)/\rho_2$, (\bar{u}_1, \bar{v}_1) and (\bar{u}_2, \bar{v}_2) are mean velocity vectors for two layers which are related with velocity vectors (u_1, v_1) and (u_2, v_2) by

$$\left. \begin{aligned} \bar{u}_1 &= \int_{-h_1}^{\eta_s} u_1 dz, \quad \bar{v}_1 = \int_{-h_1}^{\eta_s} v_1 dz \\ \bar{u}_2 &= \int_{-H}^{-h_1} u_2 dz, \quad \bar{v}_2 = \int_{-H}^{-h_1} v_2 dz \end{aligned} \right\} \quad (2)$$

Furthermore, the equations of continuity for two layers are

$$\frac{\partial \eta_s}{\partial t} = \frac{\partial \eta_i}{\partial t} - \frac{\partial \bar{u}_1}{\partial x} - \frac{\partial \bar{v}_1}{\partial y}, \quad \frac{\partial \eta_i}{\partial t} = -\frac{\partial \bar{u}_2}{\partial x} - \frac{\partial \bar{v}_2}{\partial y} \quad (3)$$

The stress τ_s (surface) and τ_b (bottom) are estimated by

$$\tau_s = 2.6 \times 10^{-3} \rho_a W |W|, \quad \tau_b = 2.6 \times 10^{-4} \rho_2 \sqrt{u_2^2 + v_2^2} - \tau_s \quad (4)$$

in which ρ_a and W are air density and wind speed.

Boundary condition is that normal components of the velocity equal zero at the boundary, and initially the surface and interface start to oscillate with no fluid motion.

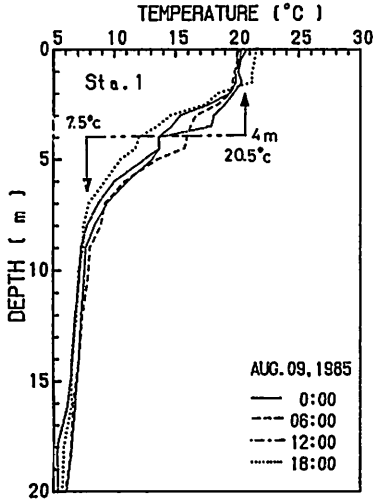


Fig. 11 Vertical profile of water temperature at Sta. 1 on 9 August, 1985.

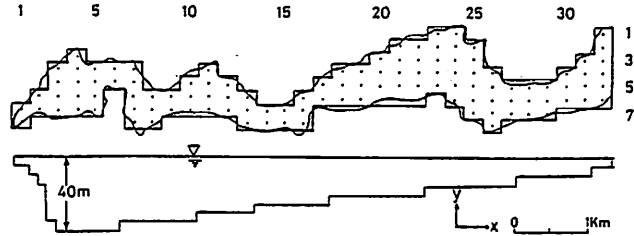


Fig. 12 Computational grids and longitudinal cross-section of model Kanayama Reservoir.

The employed values ; $h_1=4.0\text{m}$, $\rho_1=998.13\text{kg/m}^3$ and $\rho_2=999.91\text{kg/m}^3$ were obtained from the vertical distributions of the water temperature observed on 9 August shown in Fig. 11. Initial interface was taken as the mean level of the inflection points of the temperature profiles. The values of ρ_1 and ρ_2 were calculated from the water temperature of the upper and lower layer ; 20.5°C and 7.5°C . The whole reservoir was digitalized in $(N_x, N_y)=33 \times 8$ meshes as shown in Fig. 12 and equations (1) and (3) were converted into difference equations for each mesh ($\Delta x=250\text{m}$, $\Delta y=100\text{m}$) and time step ($\Delta t=3.0\text{sec}$).

In order to take account of the local wind effect through the reservoir surface, the wind recorded at Sta. 1 was assumed to act on the surface of $N_x \leq 23$, while the wind recorded at Sta. 3 for $N_x \geq 24$.

The solid lines in Fig. 13(a) and (b) show the results of the simulation using the parameters shown in Fig. 11. Dashed lines are recorded isotherms for 14°C and 18°C . This calculation shows that the amplitude of the internal motion caused by the wind action is about 3m and this result agrees with that of the field observation at Sta. 1. The good agreement can not be obtained at Sta. 3, though its dominant period of the power spectrum $T_s \approx 21\text{hr}$ is roughly equal to the field record.

(2) Period of internal seiche

As shown in the former section, it is found that the periods of the internal oscillation are obtained as 23hr 13min at Sta. 1 and 21hr 20min at Sta. 3 respectively by the spectral analysis of the observed water temperature. These values are nearly equal to the periods of the change of wind

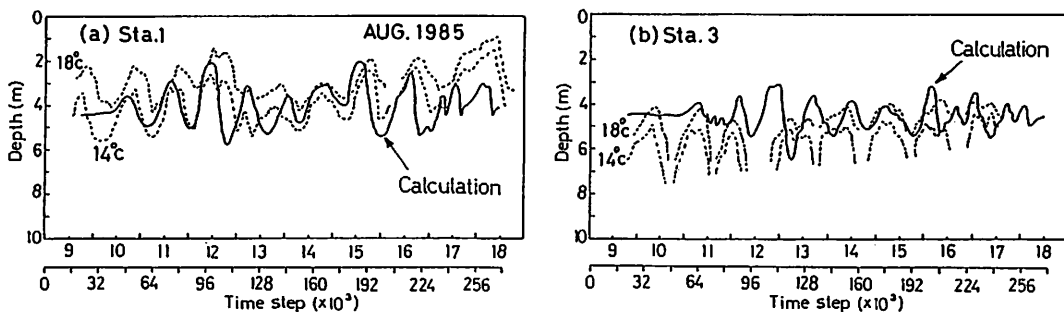


Fig. 13 Comparison between calculated and observed internal oscillations.

speed ; 23hr 16min at Sta.1 and 21hr 15min at Sta.3 . Therefore, it seems that the internal oscillation is compulsory oscillation induced by the wind force.

In order to make sure the above mentioned result, we compare the period of the internal oscillation with that of the internal seiche in this reservoir. In the observational period, it was difficult to measure the water temperature change owing to only the internal seiche because the wind blew periodically and the internal oscillation was induced by the wind force. Therefore, a calculation of a natural oscillation of the interface without the wind blow was carried out. The condition used in the calculation was that the thickness of the upper layer was 5m and the water temperature was taken as 22°C and 7°C in the upper and lower layer respectively, so that the relative density difference between two layers was $\epsilon = 2.13 \times 10^{-3}$.

The initial condition was that the SW wind of speed 5m/s had stopped to blow after continual blow for six hours. In this calculation, the similar computational method to the case of the wind-induced oscillation was used by putting the wind velocity at zero.

Figures 14(a) and 14(b) show the spectra of the calculated internal seiche at Sta.1 and Sta.3 respectively. From the figures, natural periods are indicated as 17hr 03min at Sta.1 and 18hr 57min at Sta.3 . These periods are about six and two hours shorter than the periods obtained from the water temperature changes.

From the fact that the observed internal oscillation has a nearly equal period to the wind change but different from the internal seiche, it can be shown that the internal oscillation is mainly influenced by the wind force.

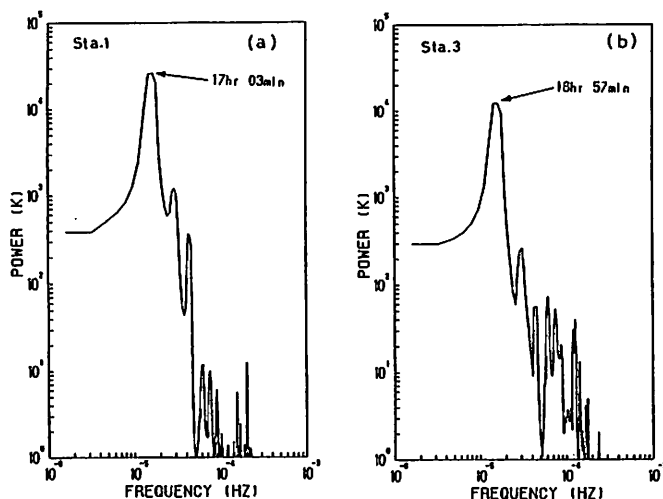


Fig. 14 Power spectra of internal seiche at Sta.1 and Sta.3 .

CONCLUSIONS

The following results are obtained as conclusions through this paper.

- (1) According to the observed results in Kanayama Reservoir which has the longitudinal section of triangular shape, the water temperature fluctuates with different amplitude and frequency at the upstream station (Sta.3) and the downstream station (Sta.1). At Sta.1 where the water depth is about 35m, the depth of the thermocline fluctuates between 3m and 5m, and the amplitude of the water temperature change reaches 10°C near the thermocline. At Sta.3, the water depth is shallower (about 12m) and the amplitude is larger compared with Sta.1. When the strong wind blows in the direction from the dam to the end of the reservoir, the temperature of the lower layer becomes nearly equal to that of the upper layer owing to the set-down of the interface.
- (2) By spectral analysis of the changes of the isothermal lines, the periods of the internal oscillation were obtained as 23hr 13min at Sta.1 and 21hr 15min at Sta.3. These periods are nearly equal to the periods of the wind speed ; 23hr 16min at Sta.1 and 21hr 20min at Sta.3.
- (3) Two-layer model was applied to simulate the internal oscillation induced by the wind. The calculated amplitude and period had a good agreement with the observed result at Sta.1. However,

the agreement was not so good at Sta.3 .

The periods of the internal seiche were calculated as 17hr 03min at Sta.1 and 18hr 57min at Sta.3 .

(4) From the results that the periods of the internal oscillation are nearly equal to those of the wind at Sta.1 and Sta.3 but different from the internal seiche, it might be concluded that the internal oscillation is a compulsory oscillation induced by the wind force.

ACKNOWLEDGEMENT

The authors would like to express their sincere thanks to the Kanayama Dam Superintendent Office of the Hokkaido Development Bureau for supplying hydrological data and Mr.K.Nakamura for his helpful support to observations.

REFERENCES

1. Fukushima,T. and Muraoka,K. : Field observation and modelling of seiche in a shallow lake, Proc. 25th Japanese Conference on Hydraulics, JSCE, pp.577-583, 1981 (in Japanese).
2. Furumoto,K., Takemasa,T., Ichinose,K. and Fujikawa,Y. : Internal seiche in density stratified lake, Proc. 29th Japanese Conference on Hydraulics, JSCE, pp.389-394, 1985 (in Japanese).
3. Heaps, N.S. and A.E. Romsbottom : Wind effects on the water in a narrow two-layered lake, Phil. Trans. Roy. Soc. London, Ser.A, Vol.259, pp.391-430 (1966).
4. Imberger,J. : The diurnal mixed layer, Limnol. Oceanogr. 30(4), pp.737-770, 1985.
5. Kanari,S. : Internal waves in Lake Biwa (II), Bull. Disas. Prev. Inst., Kyoto Univ., Vol.22, Part 2 , No.202, pp.69-96, 1973.
6. Mortimer,C.H. : Motion in the thermocline, Verh. Int. Ver. Limnol., Vol.14, pp.79-82, 1961.
7. Muraoka,K. and Hirata,T. : Observation of internal seiche and wave in thermally stratified lake, Jour. of Hydrosience and Hydraulic Engineering, Vol.2 , No.2 , pp.45-55, 1984.

APPENDIX-NOTATION

The following symbols are used in this paper;

H	=total depth (m) ;
u_1, v_1	=x and y component of flow velocity in upper layer (m/s) ;
u_2, v_2	=x and y component of flow velocity in lower layer (m/s) ;
\bar{u}_1, \bar{v}_1	=x and y component of mean velocity in upper layer (m/s) ;
\bar{u}_2, \bar{v}_2	=x and y component of mean velocity in lower layer (m/s) ;
h_1	=mean depth of upper layer (m) ;
g	=gravitational acceleration (m/s^2) ;
ρ_1	=fluid density of upper layer (kg/m^3) ;
ρ_2	=fluid density of lower layer (kg/m^3) ;
ρ_a	=density of air (kg/m^3) ;
ϵ	=relative density difference;
η_s	=surface elevation (m) ;
η_i	=interface elevation (m) ;
τ_s	=surface stress (N/m^2) ;
τ_b	=bottom stress (N/m^2) ;
w	=wind velocity vector (m/s) ;
N_x	=mesh number of x coordinate ; and
N_y	=mesh number of y coordinate.